Application of a Fibrous Shell Element Model to Bending of Pre-Gelled Unidirectional Composite

H. Courteau-Godmaire[1]*, J. Reiner[1], G. Fernlund[2] and R. Vaziri[1]
[1] Department of Civil Engineering, The University of British Columbia, Vancouver, Canada
[2] Department of Materials Engineering, The University of British Columbia, Vancouver, Canada
* Corresponding author (hubert@composites.ubc.ca)

ABSTRACT

Bending properties of uni-directional thermoset pre-preg plies influence the drape forming behavior and wrinkle morphology. Adequate modeling techniques need to account for the fibrous nature of the material, as well as the high anisotropy arising from low transverse shear and high axial stiffness. Liang *et al.* (2017) propose a degenerated shell element that decouples the bending and shear behavior of a thick interlock ply. In this paper, the shell formulation is reproduced and modified to account for transverse shear stiffness and its performance is verified against an analytical bending model proposed by Sachs and Akkerman (2017).

KEYWORDS: *Thermoset composites forming, Non-linear finite elements analysis, Ply bending behavior, Transverse shear deformation*

1 INTRODUCTION

To meet the increasing demand for composite components, hot drape forming of thermoset prepreg is favored for its manufacturing convenience and fast rate of production. The forming process imposes permanent deformations on the blank through three main modes: in-plane shear, inter-ply slip and ply bending. In order to simulate forming, these three modes have to be well characterized and modeled. While bending characterization has not received as much attention in the past, the need for more precise simulations, especially in terms of wrinkling, appeal to a better understanding of the mechanisms involved.

Classical beam theory and continuum mechanics struggle at describing the bending behavior of highly anisotropic fibrous materials (Boisse *et al.*, 2018). Development of proper mechanistic models should lead to a simpler characterization based on the behavior of the constituents only. Moreover, a representative constitutive model within an appropriate finite element formulation should provide more reliability.

Many authors propose bending models with assumptions associated with their own material type. In this paper, two of these models, namely the Liang's *et al*. (2017) shell formulation for frictionless layered fibrous media and the analytical viscoelastic bending model of Sachs and Akkerman (2017) are introduced and subsequently merged together to describe the bending behavior of multi-layer beams, made of linear elastic stiff fibres separated by soft viscoelastic layers representing the pre-gelled resin.

1.1 Liang fibrous shell

Liang's shell is based on Ahmad's shell formulation (Ahmad *et al.*, 1970) which condensates the thick shell surface degrees of freedom towards the mid-plane by introducing a rotational degree of freedom on the remaining mid-plane node.

As shown in Figure 1, the shell behavior is derived from the contribution of each fiber segment connected to the material directors, $\mathbf{V}_2$, across the thickness. Each segment has an axial and a bending stiffness, yielding a force and a moment summed up at the mid-plane node.

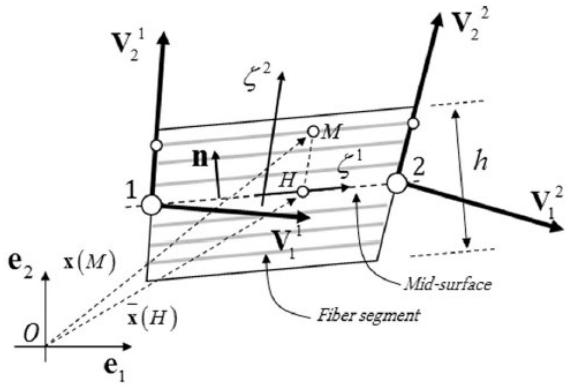

Figure 1: 2D plane strain fibrous shell element with 2 nodes on the mid-surface displaying the fiber segments connected to the material directors $\mathbf{V}_2$ (adopted from Liang *et al.*, 2017)

The bending moment is derived from the fiber segment curvature, which arises from a non-local method fitting a cubic polynomial curve through the element's neighboring nodes. It allows the overall bending of the shell to be completely independent of any material shear or rotation, which is not the case for Kirchhoff-Love or Mindlin-Reissner plates. Liang's shell is intended for thick interlock dry fabrics. Therefore, no shear interaction is introduced between the fiber segments. Namely, the fiber segments may slip past each other in a frictionless manner.

The fibrous shell is designed for single layer applications. The lack of a through-thickness description limits the potential for normal or tangential interactions with a tool or neighboring plies.

1.2 Sachs layered elastic/viscous beam

Sachs and Akkerman (2017) propose an analytical beam formulation, presented in Figure 2, based on the stack of alternating thin elastic beams and power-law viscous layers to represent the fibers and the matrix, respectively. The resulting model yields a viscoelastic beam description that captures the rate dependent nature of prepreg bending.

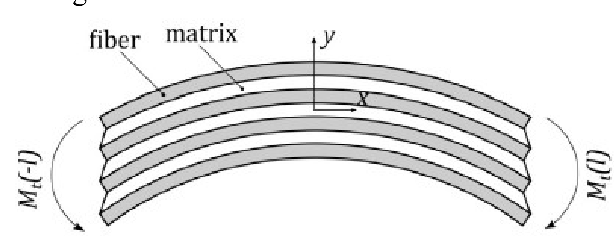

Figure 2: Layered beam model alternating classical elastic beams and viscous shear layers (adopted from Sachs and Akkerman, 2017)

Sachs and Akkerman compare this model to a series of experimental bending tests carried on a test rig schematized in Figure 3. The ply is clamped only at one end, while at the other end a gap allows for transverse shear and slip to take place. Stacks of 2, 4, or 8 plies are bent from 0° to 60° at four different constant angular velocities.

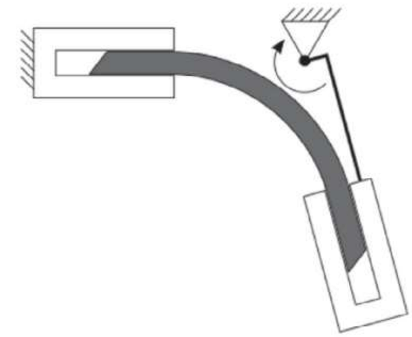

Figure 3: Diagram of Sachs bending experiment (adopted from Sachs and Akkerman, 2017)

2 CURRENT MODEL

2.1 Implementation

Liang's shell finite element method was implemented in MATLAB. Assumptions were made about damping, time step and rate of loading; otherwise, the model would suffer from typical explicit solving artifacts such as excessive numerical noise (oscillations) and divergence of the time integration.

That replication was compared to one of Liang's validation cases, which considers the bending of a 130-page softcover book clamped at its spine and undergoing self-weight loading. Figure 4 exhibits the superposition of the deflection profiles predicted by the current model (in blue) and Liang's *et al.* model (in green) at the same value of tip displacement (103 mm), where a reasonable agreement is obtained. However, when cross-sectional rotations are examined, the replicated model seems to overestimate the shear strains as measured by the angle between the mid-plane and the cross-sectional plane. It is unclear whether or not this is the outcome of the explicit solution scheme adopted.

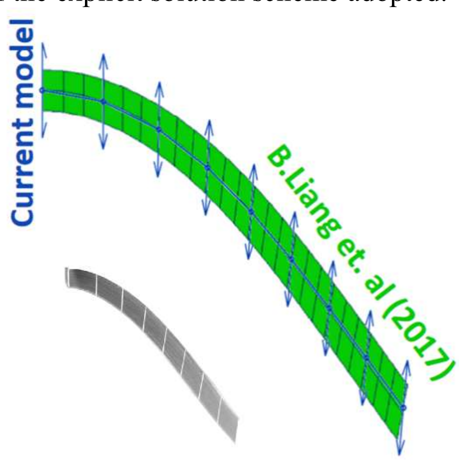

Figure 4: Curremt model (blue) overlaid on Liang's results (green) for the bending of a 130-pages softcover book clamped on the left and undergoing self-weight loading

2.2 Sachs beam model adaptation

The selected case to be reproduced was the bending of two 1mm thick plies at the slowest loading rate to limit the strain rate dependent viscous effects. Sachs assumed fiber and matrix layers of 7μm and 5μm thickness, respectively. Hence, 2 plies incorporated 167 elastic layers. Such a large number of fiber segments was computationally too costly for the fibrous shell implementation. Therefore, the thickness was instead discretized into 33 fiber segments based on equivalent 60μm thick groups of 5 fiber layers. It assumed parallel elastic beams separated by an 5μm gap layer. The effective bending stiffness B of these bundles was obtained as follows:

$$B = EI_f n_f \tag{1}$$

where E is a single elastic layer tensile modulus, I_f the 2nd moment of area of a single elastic layer, and n_f the number of layers in the group.

According to Sachs method, the boundary conditions were initially set to allow slip and shear in the right clamp while they only allowed shear in the left clamp (Figure 3). However, it had to be adapted since a large amount of slip towards the inside of the moving clamp is necessary to maintain a pure bending condition. It was more practical to allow slip in both clamps.

Before introducing a viscous shear layer between the fiber segments, a simple elastic tangential interaction was implemented. As shown in Figure 5a, it tracked the displacement of each fiber segment middle point. The relative displacement was reacted by a spring, introducing a translational force into the adjacent segments, adding up to the axial forces.

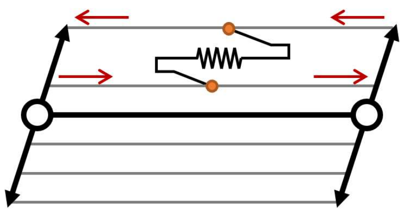

(a) Tangential spring between fiber segments

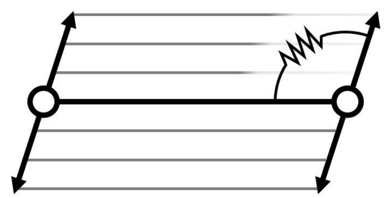

(b) Rotational spring on the material director

Figure 5: Two implementations of shear stiffness within the fibrous shell framework

After encountering issues with the first approach, described in the results section, a second approach presented in Figure 5b was developed. It connected the material director with a torsional spring to the mid-plane, providing a kinematics very similar to the first approach.

A model without shear stiffness was first ran to serve as a baseline. The elastic shear stiffness was then activated to study its effect on the macroscopic bending behavior.

3 RESULTS

Figure 6 shows the fibrous shell bent to an angle of 60°. The arrows represent the material director orientation. The fiber segments through the thickness are not displayed.

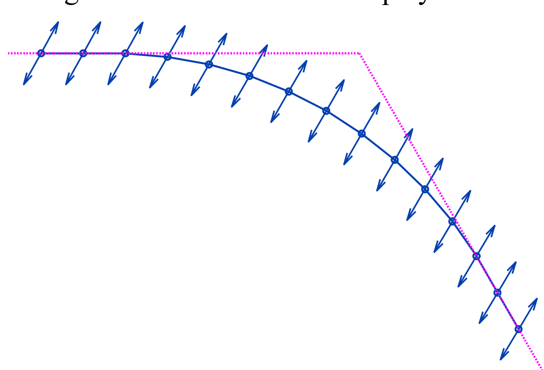

Figure 6: Fibrous shell subjected to bending, reproducing the loading conditions of Figure 3

Figure 7 shows the computed bending moment as a function of the rotation angle for both Sachs' calibrated analytical model and the Liang's fibrous shell adaptation. The latter underestimates the bending moment. That discrepancy was expected since both models do not represent the same scenario. The purely elastic fibrous shell approach offers a lower bound to Sachs model.

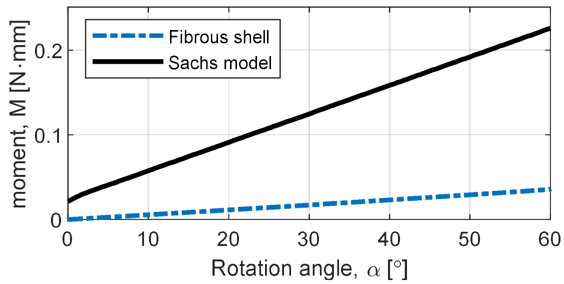

Figure 7: Comparison of moment as a function of rotation angle for Sachs analytical model and the fibrous shell implementation without shear stiffness

Next, the first shear stiffness implementation, as presented in Figure 5a was activated. It introduced numerical oscillation issues related to the analysis time step. Furthermore, the shear forces applied on the fiber segment seemed to interfere with the already existing axial forces. Overall, the first shear stiffness implementation made the model very unstable.

The second shear stiffness implementation of Figure 5b provided a more stable solution. For simple tip loaded cantilever beams, it exhibited the expected stiffening effect. The global bending stiffness could be doubled. Over that value, the model became unstable.

To explain that situation, suppose an infinite torsional stiffness. The model should retrieve the classical Bernoulli-Euler beam solution as the material director remains perpendicular to the mid-plane. The outer fiber segments would then be stretched and compressed. However, because of their special ability to bend, when compressed, the stiff fiber segments have a tendency to buckle, leading to the analysis diverging or failing to reach a stable solution. Conversely, when the axial stiffness of the segments is low, the global bending stiffness of the shell is reduced. The model independent definition of high bending and low axial stiffness allows for this non-physical scenario where it is easier for segments to compress axially rather than bend out-of-plane.

This stiffness mismatch issue led to difficulties when Sachs' conditions were reproduced. Initially, the axial stiffness was meant to be set at 230 GPa. However, in the explicit finite element method, stiffer materials impose smaller time step requirements for solution stability. The axial stiffness was therefore reduced to achieve practical computation times, while the segment bending stiffness remained unchanged. The frictionless implementation results were not affected as the segments slipped past each other and no axial stress was built up.

When shear was introduced, the axial behavior of the segments became significant again. To match Sachs' analytical model, the axial properties had to be increased to very high values, leading to very long simulation runs, which mostly aborted (diverged) because of the onset of fiber segment buckling.

4 DISCUSSION

The discrepancy presented in Figure 7 between the analytical model and the simulation without shear interaction between layers (frictionless condition of Liang *et al.*) is quite significant. The exploratory work involving the implementation of shear stiffness never seemed close to providing the missing bending stiffness.

Computation of Sachs model with very low values of viscosity could help understand the differences as the analytical model would behave more like a stack of spaced out thin elastic beams, as is the case with Liang's shell model. A good match would provide a valuable verification for the numerical model.

From a numerical method point of view, the results underscored the difficulties associated with the explicit finite element method. The high axial stiffness of carbon fibers brings down the time step for stable numerical integration, while bending and forming remain slow (long duration) processes. Furthermore, stiffness discrepancies between the different deformation modes make the model prone to excessive oscillations.

To add to the pre-existing poor computational efficiency, the fibrous shell method computes the contribution of every fiber segment. It makes the approach time consuming to a point where in terms of efficiency it would be comparable to a mesoscale model in which every fiber segment would be meshed independently.

From a physical point of view, the numerical model faced difficulties with two phenomena that are often deemed to be secondary. First, the slip boundary condition in the clamp revealed that a large amount of sliding is necessary to maintain the pure bending condition.

Secondly, the issue with fiber buckling introduced by shear stiffness is more than a numerical aberration. Rather, it is quite close to what has been observed experimentally by Farnand (2017) where the fibers within a ply would favor buckling (wrinkling and misalignment) over straining (shortening) axially in compression. What seems to transpire as a failure of the numerical model is perhaps indicative of an important ply bending compliance mechanism that should be addressed and integrated into the model. For example, the reduced load bearing capabilities of fibers could be represented by a softening model applied to their compressive stiffness.

5 CONCLUSION

The fibrous shell method proposed by Liang *et al.* (2017) was reproduced in MATLAB. Its unconventional way of handling bending with a non-local approach allowed for a complete decoupling of transverse shear and bending. This feature is critical for pre-preg bending modeling as the large transverse shear strain contributes to the overall bending compliance (i.e. in a book-like manner).

To account for the significant viscous resin contribution, the fibrous shell formulation was modified to carry non-zero transverse shear stiffness. A comparative analytical model developed by Sachs and Akkerman (2017) provided a verification case for the numerical model.

The modified model could not reproduce the analytical results due to impractical computational times associated with the small time-step size arising from the fibers high axial stiffness. Moreover, what seemed to correspond to the onset of buckling (wrinkling) when the fiber segments were compressed halted the computational run. This deformation mode has ties to physical behavior and should be addressed and considered in future models.

6 ACKNOWLEDGEMENTS

The authors acknowledge the financial contribution of the Natural Sciences and Engineering Research Council of Canada (NSERC) along with the industrial members of the Composites Research Network (The Boeing Company, Convergent Manufacturing Technologies Inc., Toray Americas, Avcorp Industries).

REFERENCES

Ahmad, S., B. M. Irons, and O. C. Zienkiewicz. (1970). Analysis of thick and thin shell structures by curved finite elements. International Journal for Numerical Methods in Engineering, Vol. 2, no. 3, pp. 419-451

Boisse P., Colmars J., Hamila N., Naouar N. and Steer Q. (2018). Bending and wrinkling of composite fiber preforms and prepregs. A review and new developments in the draping simulations. Composites Part B, Vol. 141, pp. 234-249.

Farnand K. (2016). Process-Induced Wrinkling and Waviness in Prepreg Charge-Forming. Master's thesis, University of British Columbia

Liang B., Colmars J. and Boisse P. (2017). A shell formulation for fibrous reinforcement forming simulation. Composites Part A, Vol. 100, pp. 81-96.

Sachs U. and Akkerman R. (2017). Viscoelastic bending model for continuous fiber-reinforced thermoplastic composites in melt. Composites Part A, Vol. 100, pp. 333-341.

Sachs U. (2014). Friction and Bending in Thermoplastic Composites Forming Processes. PhD thesis, University of Twente